5712 *Chem. Mater.* **2010,** *22,* 5712–5717
DOI:10.1021/cm1017954

CHEMISTRY OF MATERIALS
Article

Ten Layered Hexagonal Perovskite $Sr_5Ru_{5-x}O_{15}$ ($x = 0.90$), a Weak Ferromagnet with a Giant Coercive Field $H_c \sim 12$ T

Ayako Yamamoto,*[,†] Daisuke Hashizume,[†] Hiroko Aruga Katori,[†] Takahiko Sasaki,[‡] Eiji Ohmichi,[§] Terukazu Nishizaki,[‡] Norio Kobayashi,[‡] and Hidenori Takagi[†,⊥]

[†]*Advanced Science Institute, RIKEN, Hirosawa 2-1, Wako, Saitama, 351-0198, Japan,* [‡]*Institute for Materials Research, Tohoku University, Sendai, 980-8577, Japan,* [§]*Department of Physics, Kobe University, Kobe, 657-8501, Japan, and* [⊥]*Department of Advanced Materials, University of Tokyo, Kashiwa, 277-8561, Japan*

Received June 27, 2010. Revised Manuscript Received September 6, 2010

A single crystal of $Sr_5Ru_{5-x}O_{15}$ ($x = 0.90(2)$) with mixed valence of Ru(IV) and Ru(V) was synthesized under a high pressure of 4 GPa with an oxidizer. $Sr_5Ru_{5-x}O_{15}$ crystallizes in a hexagonal perovskite-type structure with a space group $P6_3/mmc$ (No.194), $a = 5.5600(11)$ Å, and $c = 22.830(5)$ Å. An alternative stacking of four corner-sharing (*c*) SrO_3 layers and one face-sharing (*h*) SrO_3 layer linking RuO_6 octahedra and its doubling along *c*-axis gives a 10 layer period hexagonal cell (10*H*) which is denoted by $(ccccch)_2$. The partial deficiency of Ru found in face-sharing octahedra, as reported for 8*H*-$Sr_4Ru_{4-x}O_{12}$ ($x = 0.95$) with $(ccch)_2$ stacking, yields an average Ru valence estimate of 4.87. The bond valence analysis indicates that the valence of Ru in fully corner-sharing octahedra is nearly 5, while that of Ru in face-sharing octahedra is considerably lower than 5. This compound is a weakly ferromagnetic metal with Curie temperature $T_c = 160$ K and a saturated moment of 0.07 and 0.05 μ_B/Ru in $H \perp c$ and $H \parallel c$, respectively. In the ferromagnetic state, we found remarkable enhancement of the coercivity below 50 K. At 1.7 K, a giant coercive field of ~12 T was observed. We argue that Ru(IV,V) in face-sharing layers are responsible for the ferromagnetism and that possible glassy character due to frustration and disorder may at least in part contribute to the giant coercivity.

The 4d electrons of ruthenium are known to exhibit both localized and itinerant characters. The subtle balance between localization and itinerancy can be modified by the crystal structure and the valence state of Ru, giving rise to a rich variety of electronic and magnetic properties. In the Sr−Ru(IV)−O system, for example, Sr_2RuO_4[1] in the Ruddlesden−Popper series ($Sr_nRu_{n-1}O_{3n-2}$, $n = 2$) is a paramagnetic metal and shows superconductivity at 1.5 K. $Sr_3Ru_2O_7$[2] ($n = 3$) is also a paramagnetic metal but shows a metamagmetic transition, indicative of close proximity to magnetic order. In addition, $SrRuO_3$[3] ($n = \infty$, perovskite type) is a ferromagnetic metal (Curie temperature, $T_c = 160$ K). All these compounds have a stacked square-lattice structure consisting of corner-shared network of RuO_6 octahedra.

By introducing Ru(V) which can be usually stabilized under a high oxygen pressure[4−6] or hydroxide melts,[7] one can widen the structural varieties and find not only corner-sharing but also edge- and face-sharing RuO_6 octahedra. $Sr_4Ru(V)_2O_9$,[4] for example, has a pseudo one-dimensional structure with face-sharing octahedral, whereas $Sr_2Ru(V,VI)_3O_{10}$[5] has a rutile-related structure in which edge-sharing octahedra are realized. Magnetic and electronic properties of such Ru(V)-including compounds with distinct structural features are, thus, quite attractive in view of a possible interplay of itinerant and localized character of Ru 4d electrons which can give rise to phase transitions.

A decade ago, a perovskite related compound, 8*H*-$Sr_4Ru(V,VI)_{4-x}O_{12}$[6] was reported to crystallize with an eight layer period hexagonal (8*H*) cell in which face-sharing RuO_6 layers were inserted into $SrRuO_3$ perovskites. This compound falls into the category of so-called hexagonal perovskite, $A_{n-x}B_{n-y}O_{3n-d}$,[8] which is described by the stacking sequence of corner-sharing (c) and face-sharing (*h*) closed packing AO_3 layers. $Sr_4Ru_{4-x}O_{12}$ can be accordingly described as $(ccch)_2$. Such a hexagonal perovskite, e.g., $BaFeO_3$ ($(cch)_2$), $BaNiO_3$ (*h*), often appears when the tolerance factor for ABO_3

*To whom correspondence should be addressed. Fax: +81 48 462 4649. Tel: +81 48 462 1111(ex. 8756). E-mail: ayako-yamamoto@riken.jp.

(1) Maeno, Y.; Hashimoto, H.; Yoshida, K.; Nishizaki, S.; Fujita, T.; Bednorz, J. G.; Lichtenberg, F. *Nature* **2002**, *372*, 532.
(2) Ikeda, S.-I.; Maeno, Y.; Nakatsuji, S.; Kosaka, M.; Uwatoko, Y. *Phys. Rev. B* **2000**, *62*, R6089.
(3) (a) Callaghan, A.; Moeller, C. W.; Ward, R. *Inorg. Chem.* **1966**, *5*, 1572. (b) Jones, C. W.; Battle, P. D.; Lightfoot, P.; Harrison, W. T. A. *Acta Crystallogr.* **1989**, *45C*, 365.
(4) Dussarrat, C.; Fompeyrine, J.; Darriet, J. *Eur. J. Solid State Inorg. Chem.* **1995**, *32*, 3.
(5) Renard, C.; Daviero-Minaud, S.; Abraham, F. *J. Solid State Chem.* **1999**, *143*, 266.
(6) Renard, C.; Daviero-Minaud, S.; Huve, M.; Abraham, F. *J. Solid State Chem.* **1999**, *144*, 125.
(7) For example, Gemmill, W. R.; Smith, M. D.; Loye, H.-C. *Inorg. Chem.* **2004**, *43*, 4254.
(8) Wells, A. F. In *Structual Inorganic Chemistry*, 5th, ed.; Oxford Univ. Press: Oxford, 1984; Chapter 13, pp 574.

 Published on Web 09/28/2010

perovskite, t, ($t = (r_A+r_O)/(2)^{1/2}(r_B+r_O)$, where r is an effective ionic radius), is larger than 1.00. Therefore, it may be natural that a hexagonal perovskite structure is stabilized in $Sr_4Ru(V,VI)_{4-x}O_{12}$ with $t \sim 1.04$. Another distinct structural feature of $Sr_4Ru_{4-x}O_{12}$ is that the occupancy of Ru in face-sharing octahedra is only about 50%, probably due to the strong electrostatic repulsion between the two types of Ru ions.

Stimulated by this investigation, we have carefully explored closely related Sr−Ru−O compounds using a high-pressure method. Here, we report the synthesis, crystal structure, and physical properties of a new hexagonal perovskite, 10*H*-$Sr_5Ru_{5-x}O_{15}$, with $(cccch)_2$ stacking. We found a weak ferromagnetism below 160 K with an extremely high coercivity $H_c \sim 12$ T at 1.7 K.

Experimental Section

The samples were prepared from an equimolar mixture of anhydrate $Sr(OH)_2$ (99.995%, Sigma-Aldrich, dried at 100 °C) and RuO_2 (99.9%, Kojundo Chemical CO., dried at 350 °C) with an oxidizer, $KClO_3$ (99.99%, Sigma-Aldrich, ca. 15% weight of total mixture). The pelletized powder was sealed in a gold cell (3.5 mm in diameter and 6.4 mm in height) and then assembled into a pyrophyllite cube together with a carbon tube-heater and an insulating boron nitride sleeve. It was heated at 950 °C for 0.5−2 h under 4 GPa using a cubic anvil-type high-pressure apparatus (TRY engineering Co., CA 180P). Two kinds of microcrystal were obtained together with RuO_2 (unreacted) and KCl (the decomposition of $KClO_3$). The two types of crystal could be distinguished very easily by the shape. The thermal stability was examined by thermogravimetricmeter (Mac Science) in flowing oxygen gas (99.999%). The magnetic property of these crystals was measured after washing in diluted HCl aqueous solution. Compositional analyses were carried out by an inductively coupled plasma (ICP, Shimadzu ICPS-1000IV), electron probe microanalyzer (EPMA, JEOL, JXA-8200), and energy dispersive X-ray analyzer (EDX, JEOL, JED-2200) combined with a scanning electron microscope (SEM, JEOL, JSM-6330F).

Structural data for a platelike black single crystal ($0.12 \times 0.08 \times 0.03$ mm^3) were collected on a diffractometer (RIGAKU AFC-8) equipped with a CCD detector (Saturn70) with Mo Kα radiation by an oscillation method at 300 K. The initial structure of the crystal was solved by a direct method using the programs SHELXS97[9] and refined by a full matrix least-squares method using the program SHELXL97.15.[9] The detail is described in the CIF (Supporting Information).

The electrical resistivity and the specific heat were measured using a physical property measurement system (Quantum Design, PPMS). The susceptibility (-1 T $< H <$ 1 T) was measured with a superconducting quantum interference device (SQUID) magnetometer (Quantum Design, MPMS) using 20 crystals glued to a high purity aluminum plate with the crystal plane parallel to the plate. For measurements of magnetic property at higher magnetic field, the following instruments are used (i) a vibrating sample magnetometer (superconducting magnet, -12 T $< H <$ 12 T, Oxford VSM), (ii) a torque meter with a cantilever (superconducting magnet, -15 T $< H <$ 15 T and hybrid magnet, 0 T $< H <$ 27 T, Institute of Materials Research, Tohoku Univ.), and (iii) a torque meter with a cantilever (a pulse high-field generator, -23 T $< H <$ 33 T, Kobe Univ.).

(9) Sheldrick, G. M. *Acta Crystallogr.* **2008**, *64A*, 112.

Results and Discussion

1. Synthesis, Composition, and Structure. The first key process to obtain new Sr−Ru−O compounds with Ru(V) was the stabilization of a higher oxidation state while keeping a nearly equimolar ratio of Sr and Ru. Starting from SrO and RuO_2 together with an oxidizer $KClO_3$ provided only $SrRuO_3$ which is a typical Ru(IV) oxide. Using $Sr(OH)_2$ instead of SrO, however, two types of crystals, apparently different from $SrRuO_3$, were obtained as described below. This may result from a hydrothermal reaction occuring in a closed and high-pressured cell with water supplied by the hydroxide. $Sr_4Ru_{4-x}O_{12}$ with homologous structure of our new compound is also obtained by hydrothermal reaction. The pH may depend on the nominal ratio of $Sr(OH)_2$. Actually, a ratio of product and crystal size depended on the nominal ratio of RuO_2 and $Sr(OH)_2$. In comparison, starting from $Ca(OH)_2$, RuO_2, and the oxidizer resulted in polycrystalline $Ca_2Ru_2O_7$ with pyrochlore-type structure. Further experiments are needed to investigate how the hydroxide works in the reaction.

SEM observation of the sample revealed that the product consists of black platelike crystals (typically, hexagonal shape, $\sim 150 \times 150 \times 10$ μm^3; see the inset of Figure 3c) and black rodlike crystals (typically, $\sim 300 \times 50 \times 50$ μm^3). The EPMA analysis indicated metal ratios of Sr/Ru = 1.00:0.82 and Sr/Ru = 1.00:3.44 for plate- and rodlike crystals, respectively. These results agreed reasonably with those from EDX and ICP analyses. No incorporation of K and Cl in the crystals was found in EPMA.

The rodlike crystals were found to have a triclinic cell with space group $P\bar{1}$ (No. 2), $a = 6.6408(10)$ Å, $b = 7.3386(11)$ Å, $c = 7.4398(16)$ Å, $\alpha = 82.372(9)$ °, $\beta = 84.468(10)$ °, and $\gamma = 60.481(7)$ ° with a composition of $Sr_2Ru_7O_{18}$ from single crystal X-ray diffraction (XRD) analysis. The structure was isomorphous with $Ba_2Ru_7O_{18}$[10] prepared by the hydrothermal method. The details of structure and properties of $Sr_2Ru_7O_{18}$ will be described elsewhere.

The powder XRD pattern on the crushed powder of the platelike crystals could be indexed by assuming a layered structure in hexagonal unit cell, with $a \sim 5.56$ Å and $c \sim 11.4$ or 22.8 Å, as shown in Supplemental Figure 1 (Supporting Information). A few weak peaks from RuO_2 (starting material) and KCl (a decomposition product of oxidizer, $KClO_3$) and a trace of peaks from unknown origin are observed; the amount of RuO_2 depended on the batches, but no $SrRuO_3$, Sr_2RuO_4, $Sr_3Ru_2O_7$, $Sr_4Ru_{4-x}O_{12}$, and $Sr_2Ru_7O_{18}$ were found in the patterns. A single crystal XRD pattern was consistent with this cell. We then examined various perovskite-based structural models with different stacking as shown in Figure 1a $(chhch)_2$ as in 10*H*-$BaRuO_3$,[11] Figure 1b $(ccchh)_2$ as in 10*H*-$BaLa_4Ti_4O_{15}$,[12] and Figure 1c $(cccch)_2$ stacking. We found that the $(cccch)_2$ model provided the most reasonable fit to XRD data. Refined structural parameters and interatomic distances/angles are listed in

(10) Sato, H.; Ogawa, T.; Okuda, N.; Wakabayashi, J. *J. Phys. Soc. Jpn.* **2003**, *72*, 3035.
(11) Ogawa, T.; Sato, H. *J. Alloys Compd.* **2004**, *383*, 313.
(12) Harre, N.; Mercurio, D.; Trplliard, G.; Frit, B. *Mater. Res. Bull.* **1998**, *33*, 1537.

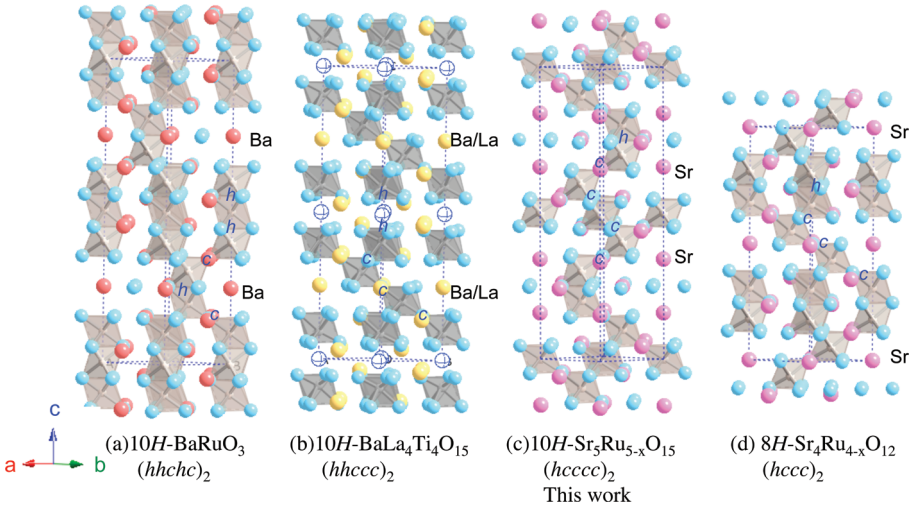

Figure 1. Schematic crystal structure models of 10*H* and 8*H* hexagonal perovskite oxides. Octahedra represent $RuO_6(TiO_6)$ that are connected by face sharing (*h*) and corner sharing (*c*).

Table 1. Refined Structural Parameters of $Sr_5Ru_{5-x}O_{15}$ at 300 K[a]

atom	site	*g*	*x*	*y*	*z*	U_{eq} (Å^2)
Ru(1)	2*a*	1.0	0	0	0	0.0045(5)
Ru(2)	4*f*	1.0	0.3333	0.6667	0.09957(6)	0.0060(4)
Ru(3)	4*f*	0.553(8)	0.3333	0.6667	0.69946(11)	0.0087(8)
Sr(1)	2*c*	1.0	0.3333	0.6667	0.25	0.0123(6)
Sr(2)	4*e*	1.0	0	0	0.15875(9)	0.0250(6)
Sr(3)	4*f*	1.0	0.3333	0.6667	0.55343(8)	0.0123(5)
O(1)	12*k*	1.0	0.5076(12)	0.015(2)	0.6465(4)	0.037(3)
O(2)	12*k*	1.0	0.1682(14)	0.336(3)	0.0462(5)	0.047(3)
O(3)	6*h*	1.0	0.8308(15)	0.662(3)	0.25	0.029(3)

[a] Space group $P6_3/mmc$ (#194), a = 5.5600(11) Å, c = 22.830(5) Å, V = 611.2(2) Å^3, R_{wp} = 5.51%, and S (goodness of fit) = 1.33. CIF for $Sr_5Ru_{5-x}O_{15}$ is available in the Supporting Information.

Table 2. Selected Bond Distances and Angles of $Sr_5Ru_{5-x}O_{15}$ at 300K, and Bond Valence Sum[14] for Each Site of Metals

bond	distance (Å)/ angle (deg)	multiplicity	bond valence sum
Ru(1)−O(2)	1.933(11)	6	Ru(1) 5.41
Ru(2)−O(1)	1.869(10)	3	
Ru(2)−O(2)	2.003(10)	3	Ru(2) 5.45
Ru(3)−O(3)	1.957(12)	3	
Ru(3)−O(1)	2.068(10)	3	Ru(3) 4.41
Sr(1)−O(3)	2.7801(6)	6	
Sr(1)−O(1)	2.816(11)	6	Sr(1) 1.91
Sr(2)−O(3)	2.645(9)	3	
Sr(2)−O(1)	2.7950(11)	6	
Sr(2)−O(2)	3.038(14)	3	Sr(2) 1.94
Sr(3)−O(1)	2.707(12)	3	
Sr(3)−O(2)	2.775(14)	3	
Sr(3)−O(2)	2.7849(9)	6	Sr(3) 2.10
Ru(1)−Ru(1)	3.933(7)	6	
Ru(2)−Ru(1)	3.933(7)	3	
Ru(2)−Ru(3)	3.937(7)	3	
Ru(3)−Ru(3)	2.307(5)	1	
Ru(1)−O(2)−Ru(1)	175.6(8)		
Ru(2)−O(1)−Ru(3)	179.2(7)		
Ru(3)−O(3)−Ru(3)	72.3(5)		

Tables 1 and 2. Note that the partial deficiency of Ru exists in face-sharing RuO_6 as in $Sr_4Ru_{4-x}O_{12}$.[6] The composition obtained by the refinement of XRD was $Sr_5Ru_{4.10(2)}O_{15}$, in good agreement with the chemical analysis. This yields an averaged valence of Ru to be 4.87. We have tried to synthesize samples with different values of x by changing the synthesis temperature and nominal composition of Sr/Ru. However, the obtained crystals always resulted in constant lattice and reproducible magnetic properties with negligible change (within error bars) for all samples. Therefore, it is concluded that x = 0.90(2) is the only stable composition, at least for samples prepared at a pressure of 4 GPa. However, we cannot be certain that the ruthenium deficiency is homogeneous on a microscopic level. We note that the difference in the standard deviation for the x and y parameters can be accounted for when the anisotropy of displacement parameter, U, is taken into account.

Thermogravimetric analysis (TGA) of the powdered $Sr_5Ru_{4-x}O_{15}$ indicated that weight loss started at 540 °C and continued to 780 °C with a narrow plateau at 650 °C in flowing oxygen gas at ambient pressure. The XRD pattern of the sample heated up to 850 °C revealed that $Sr_5Ru_{5-x}O_{15}$ transforms to $SrRuO_3$ and a small amount of SrO. Total weight loss of 2.0% should correspond to the oxygen loss by the reduction from Ru(V) to Ru(IV), indicative of the presence of Ru(V) in $Sr_5Ru_{5-x}O_{15}$. This also proves that there is no incorporation of an extra hydroxyl group attribute to the starting material $Sr(OH)_2$

Figure 2a shows the local structure of $Sr_5Ru_{5-x}O_{15}$ in comparison with that of $SrRuO_3$ (Figure 2b). The averaged Ru−O bond length for Ru(1) and Ru(2) in the fully corner-sharing octahedra is 1.933 Å and 1.936 ((1.869 + 2.003)/2) Å, respectively, which are distinctly shorter than that of $SrRuO_3$,[3b] 1.984 Å. The distance of Ru(1)/Ru(2)−O, ~1.94 Å, corresponds to pentavalence in an empirical relationship[13] between Ru−O distance and the oxidation state of Ru. The bond valence sum study,[14] an estimation method of valence

(13) Stizer, K. E.; Smith, M. D.; Gemmill, W. R.; Loye, H.-C. *J. Am. Chem. Soc.* **2002**, *124*, 13877.

(14) (a) Brown, I. D.; Altermatt, D. *Acta Crystallogr.* **1985**, *41B*, 244. (b) Brese, N. E.; O'Keeffe, M. *Acta Crystallogr.* **1991**, *47B*, 192. (c) Santoro, A.; et al. *J. Solid State Chem.* **2000**, *151*, 245. Bond valence sum, V_i, is given the formula, $V_i = \Sigma j \exp((R_0 - R_{ij})/0.37)$ (R_0, the constant value for each cation−anion combination determined by the empirical data, and R_{ij}, bond distance obtained by the structural analysis of a target compound). V_{Ru} and V_{Sr} were calculated using R_0 = 1.895 for $Ru^{5+}-O^{2-}$ and R_0 = 2.118 for $Sr^{2+}-O^{2-}$.

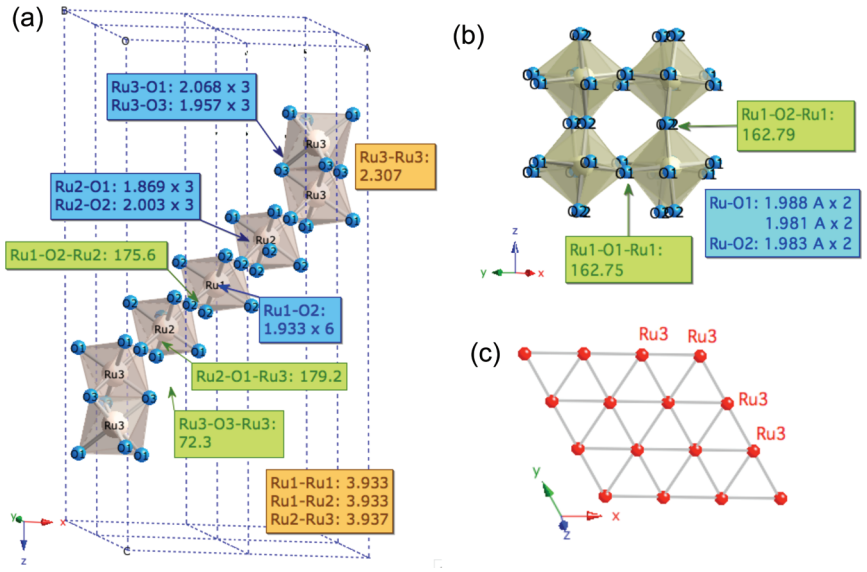

Figure 2. Local coordination of Ru−O octahedra and their bond lengths(Å)/angles(°) as measured for (a) $Sr_5Ru_{5-x}O_{15}$ and (b) $SrRuO_3$ and (c) a top view of the Ru(3) layer in $Sr_5Ru_{5-x}O_{15}$.

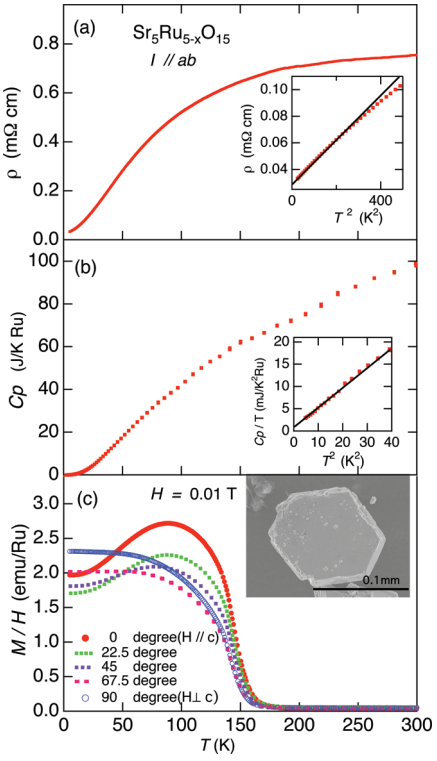

Figure 3. Temperature dependence of (a) electrical resistivity, (b) specific heat, and (c) susceptibility for $Sr_5Ru_{5-x}O_{15}$. Inset of (c) shows SEM photo of single crystal. Cp and M/H expressed per mol of Ru, assuming $x = 0.90$.

from the bond distances, also supported that both Ru(1) and Ru(2) are higher than 5, while Ru(3) is considerably lower than 5, as listed in Table 2. The bond angles of corner-sharing linking, Ru(1)−O(2)−Ru(2) and Ru(2)−O(1)−Ru(3), are 175.6° and 179.2°, respectively, which are close to the ideal angle of 180°. This indicates the local coordination of the octahedra in $Sr_5Ru_{5-x}O_{15}$ is almost free from internal stress, in contrast to the case for $SrRuO_3$ where the strong bending of the Ru−O−Ru bond by 162.79° is observed.[3b]

The face-sharing layer RuO_6 octahedra, where Ru is located in a triangular lattice as shown in Figure 2c, are structurally distinct from the fully corner-sharing octahedra. About 45% of Ru(3) was found to be deficient in the structural analysis. It may be ascribed to an electrostatic repulsion between Ru(3)−Ru(3) atoms placed with considerably short distance, 2.308 Å. Similar deficiency of cations was seen also in 8*H*-$Sr_4Ru_{4-x}O_{12}$[6] and 10*H*-$La_4BaTi_4O_{15}$[12] with double and triple face-sharing layers, respectively (cf. Figure 1d,b). In the case of 8*H*-$Sr_4Ru_{4-x}O_{12}$, the two facing Ru sites are not equivalent, while in 10*H*-$Sr_5Ru_{4.1}O_{15}$, the two appear equivalent. We argue that the cation vacancies are randomly distributed because of the rapid quenching from a high temperature. Post annealing might induce an ordering of Ru vacancy as observed in $Sr_4Ru_{4-x}O_{12}$.[6] We treat Ru(3) as one crystallographic site in this work. The bond distances of Ru(3)−O(1) and Ru(3)−O(3), ~2.00 Å, are much longer than those of Ru(1)−O and Ru(2)−O, indicating that the valence state of Ru(3) is lower than five and likely close to four. Assuming that the valence state of Ru(1) and Ru(2) is 5, that of Ru(3) is estimated to be 4.55 from the charge neutrality, which yields an averaged effective charge of 2.50 at the Ru(3). It agrees reasonably with the empirical estimate for Ru(3)−Ru(3) distance in face-sharing octahedra.[13] Such an irregular coordination may play a role as a buffer to adjust the charge and the structure in this compound.

As described above, the tolerance factor of $SrRu(V)O_3$, $t = 1.04$, is larger than the ideal value $t = 1.00$ but definitely smaller than that of $BaRu(V)O_3$ ($t = 1.10$). This should give rise to a corner-sharing rich hexagonal perovskite structure as compared with the Ba analogue. In fact, 10*H*-$Sr_5Ru_{5-x}O_{15}$ has the stacking of $(ccccch)_2$ ($c/(c + h) = 0.8$), while 10*H*-$Ba_5Ru_{5-x}O_{15}$[11] has face-sharing-rich stacking $(chhch)_2$ (=0.4). It may be natural to anticipate that the structure of $Ba_{1-x}Sr_xRuO_3$[15] would gradually change with increasing

(15) Longo, J. M.; Kafalas, J. A. *Mater. Res. Bull.* **1968**, *3*, 687.

x from the face-sharing rich phases $9H(chh)_3$, $4H(ch)_2$, and $6H(cch)_2$ to $3C((c)$: cubic perovskite) with only a corner-sharing phase. From a viewpoint of pressure, it is important to note that the synthesis pressure of $8H$-$Sr_4Ru_{4-x}O_{12}$[6] (0.18 GPa) was much lower than that of $10H$-$Sr_5Ru_{5-x}O_{15}$ (4.0 GPa). This suggests that the homologous series $Sr_nRu_{n-x}O_{3n}$ (n = 6, 7, ...) may be synthesized by applying higher pressure, as is known in the transformation from $9H$ to $3C$ for $BaRuO_3$.[16]

2. Electronic, Thermal, and Magnetic Properties. Figure 3 demonstrates the physical properties of $Sr_5Ru_{5-x}O_{15}$, indicating that the ground state is a weakly ferromagnetic metal. The temperature dependence of in-plane electrical resistivity showed a metallic behavior with T^2 dependence at low temperatures and a clear signature of resistivity saturation above 100 K, as seen in Figure 3a. Such a metallic behavior is similar to those of $SrRuO_3$[3] and $3C$-$BaRuO_3$[16] with simple perovskite structure only with corner-sharing octahedra but contrasts with those of $10H$-and $9H$-$BaRuO_3$[10,17] with face-sharing-rich structure, where the resistivity shows almost no temperature dependence with a slight upturn at low temperature. This very likely suggests that the corner-sharing Ru_3O_9 blocks in $Sr_5Ru_{5-x}O_{15}$ are responsible for the metallic conductivity. Out-of-plane resistivity could not be measured due to an insufficient thickness for the transport measurement. The specific heat, measured as a function of temperature, is shown in Figure 3b. No peak was observed around magnetic transition. This may be due to a small saturation value that is only 2% of full moment as shown below and the dominance of the lattice contribution to the heat capacity above 100 K. The electronic specific heat coefficient, γ, was estimated to be 1.5 mJ/Ru K^2 from the low temperature specific heat (inset of Figure 3b), which is comparable to those of a typical metal.

As shown in Figure 3c, the temperature dependence of magnetization with H = 0.01 T showed a weakly ferromagnetic behavior below 160 K. Normal ferromagnetic behavior, with a monotonic increase of magnetization upon cooling, is observed for $\perp c$, while a bump is observed around 80 K for H // c, suggestive of a ferrimagnetic character with complex interplay of sublattice magnetization. Analogous behavior was also reported in $Sr_4Ru_{4-x}O_{12}$.[6] A Curie−Weiss fitting of the magnetic susceptibility above $T_c \sim 160$ K gives an estimate of effective magnetic moment $P_{eff} \sim 2.82\ \mu_B$/Ru and $\Theta \sim -290$ K. P_{eff} is smaller than the expected value($P_{exp} \sim 3.87\ \mu_B$/Ru) for a S = 3/2 Ru(V) ion with g = 2. This can be attributed to a partially itinerant character of Ru d electrons. It is noted here that we have carefully considered the possibility of ferromagnetism due to a minor inclusion of the well-known ferromagnet, $SrRuO_3$ with $\sim 1.3\ \mu_B$ /Ru at 5 K.[18] Since the magnetization of the present sample at low temperature is 0.05−0.07 μ_B/Ru, if

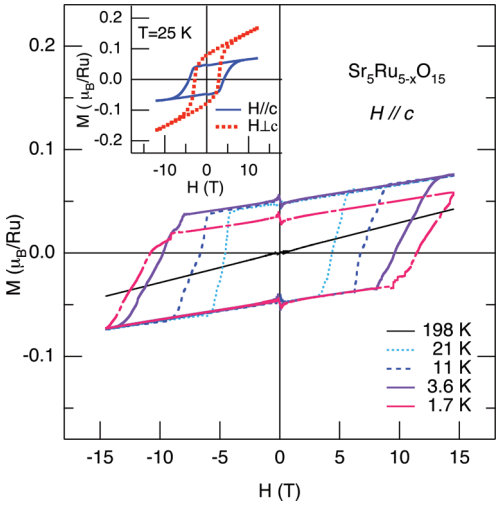

Figure 4. Temperature dependence of magnetization hysteresis loops for $Sr_5Ru_{5-x}O_{15}$. The inset figure shows hysteresis loops for H // c and $H \perp$ c at 25 K.

$Sr_5Ru_{5-x}O_{15}$ was nonmagnetic and all the magnetization was generated by $SrRuO_3$, about 5% of the sample should be $SrRuO_3$. If this was the case, it would have been easily detected in our X-ray diffraction results. However, no trace of $SrRuO_3$ was observed in both powder and single-crystal X-ray diffraction. More significantly, the anisotropy of hysteresis loop also indicates that the ferromagnetism cannot be attributed to $SrRuO_3$ due to its cubic symmetry, as described below.

An extraordinarily large coercivity was observed for the weak ferromagnetism below 50 K. In the inset of Figure 4, the magnetization hysteresis (M-H) loops up to 12 T with $H \perp c$ and H // c at 25 K shown, which indicates that the saturated moment is $\sim 0.07\ \mu_B$/Ru and $\sim 0.05\ \mu_B$/Ru for $H \perp c$ (H // a−b plane) and H // c ($H \perp a$−b plane), respectively. In accord with the temperature dependence of magnetization, we observe clear anisotropy between $H \perp c$ and H // c. Detailed results on M-H loops with various temperatures are summarized in Supplemental Figure 2 (Supporting Information), which shows a M-H loop has not been completed for H // c at 10 K. Here, let us focus on H // c. Other M-H loops up to 15 T are shown in Figure 4. At 21 K, the coercive field, H_c, is 5 T, which is already quite a large value. Remarkably, the coercive field keeps increasing very rapidly on cooling from 21 to 3.6 K, and at 1.7 K, the M-H curve up to 15 T is asymmetric, meaning that the hysteresis loop has not completely saturated even up to 15 T. Hence, H_c is, thus, at least 12 T, a truly giant value and which is to our knowledge, the largest among those reported so far for any ferromagnet. The temperature dependence of H_c determined by the M-H loops was summarized in Figure 5. Even at around 10 K, H_c is enhanced to over 5 T. In a separate torque measurement under pulse fields shown in Supplemental Figure 3 (Supporting Information), we observed hysteresis that persists at least up to 20 T at T = 1.5 K in inset panel of the figure, consistent with the results of other magnetization measurements. We also found that the irreversibility field

(16) Jin, C.-Q.; Zhou, J.-S.; Goodenough, J. B.; Liu, Q. Q.; Zhao, J. G.; Yang, L. X.; Yu, Y.; Yu, R. C.; Katsura, T.; Shatskiy, A.; Ito, E. *Proc. Natl. Acad. Sci.* **2008**, *105*, 7115.
(17) Rijssenbeek, J. T.; Jin, R.; Zadorozhny, Yu.; Liu, Y.; Batlogg, B.; Cava, R. J. *Phys. Rev. B* **1999**, *59*, 4561.
(18) Yamaura, K.; Young, D. P.; Takayama-Muromachi, E. *Phys. Rev. B* **2004**, *69*, 024410.

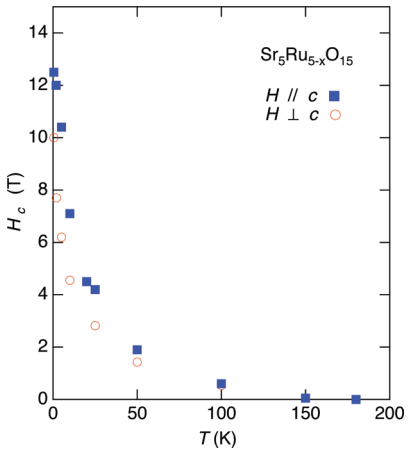

Figure 5. Summary of temperature dependent coercive force of $Sr_5Ru_{5-x}O_{15}$.

can be enhanced to 22 T by tilting the field slightly (~12°) from the *c*-axis.

At this stage, the origin of the giant H_c is not clear at all. The analysis of local structure discussed above suggests that d electrons from Ru(1) and Ru(2) sites are itinerant and give rise to the metallic transport. The magnetism likely arises from d electrons on Ru(3) sites in the face-sharing octahedral. From charge neutrality, approximately 13% of Ru should be Ru(IV) which appears to preferably occupy Ru(3) site, together with 42% of Ru(V) and 45% of vacancy. A detailed neutron diffraction study is required to determine the magnetic structure.

Recently, some organic and oxide magnets were reported to show a large coercivity over 5 T. Cobalt-radical polymer, $[Co(hfac)_2BPNN]$ (BPNN = butoxyphenyl-nitronyl nitroxide),[19a] with one-dimensional Ising chains shows a high coercive field of 5.2 T at 6 K. An extraordinary H_c value of 9 T was reported in a single crystal of a ferromagnet $LuFe_2O_4$ at 4 K.[19b] These H_cs are larger than the H_c of Sm−Co and Nd−Fe−B magnets.[20] However, these are not directly comparable, since the magnets were measured at room temperature. It is interesting that these two high coercive ferromagnets share common features with $Sr_5Ru_{5-x}O_{15}$, including the drastic enhancement of coercivity at very low temperature and the presence of geometrical frustration due to triangular geometry. Further inspections of these common features, we believe, are required to capture the essential ingredient of the enhanced coercivity of these ferromagnets.

(19) (a) Ishii, N.; Okamura, Y.; Chiba, S.; Nogami, T.; Ishida, T. *J. Am. Chem. Soc.* **2008**, *130*, 24. (b) Wu, W.; Kiryukhin, V.; Noh, H.-J.; Ko, K.-T.; Park, J.-H.; Ratcliff, W., II; Sharma, P. A.; Harrison, N.; Choi, Y. J.; Horibe, Y.; Lee, S.; Park, S.; Yi, H. T.; Zhang, C. L.; Cheong, S.-W. *Phys. Rev. Let.* **2008**, *101*, 137203.

Summary

A new 10*H* perovskite, $Sr_5Ru_{5-x}O_{15}$ ($x \sim 0.90$), was synthesized using a high-pressure technique with an oxidizer. $Sr_5Ru_{5-x}O_{15}$ crystallizes in a hexagonal system with $a = 5.5600(11)$ Å and $c = 22.830(5)$ Å, where an alternative stacking of a one face-sharing layer and four corner-sharing layers $(ccccch)_2$ is realized. We found that $Sr_5Ru_{5-x}O_{15}$ is a weakly ferromagnetic metal with a magnetic transition $T_c \sim 160$ K. Most notably, a giant coercive field of 12 T was observed, the largest known so far, which may provide us a strategy to design a highly coercive magnet.

Acknowledgment. We thank Dr. M. Uchida for structural study, Dr. K. Fujiwara and Mr. D. Hirai for resistivity measurement, and Ms. Kariya for chemical analysis. We also thank Dr. A. Chainani and Dr. A. Bangura for the English suggestions. This work was supported by Grant-in-Aid for Scientific Research (C, No. 20550135 and Priority Areas, No. 19052008) and RIKEN-ASI fund.

Supporting Information Available: Powder X-ray diffraction (PDF), magnetization (PDF), irreversible field (PDF), and crystallographic information files (CIF). This material is available free of charge via the Internet at http://pubs.acs.org.

(20) For example, in a products catalog of NeoMag Co., Ltd. (www.neomag.jp), Nd-Fe-B (Neo38EH, $H_{cj} > 30$ kOe (corresponds to 3.0 T) at RT) and Sm-Co (SS30H, $H_{cj} > 24$ kOe (corresponds to 2.4 T) at RT).